Sankara Narayanan mail id: sankaranarayanan2910@gmail.com

Incompressible blood flow in 3D straight Vein and comparing it with healthy vein using PINNs

Sankara Narayanan
Independent Student Researcher, Silvassa, Dadra and Nagar Haveli and Daman and Diu, Indiab

ARTICLE INFO

Article history:
Received
Received in revised form
Accepted

Available online

Keywords:
Physics-informed neural networks; Blood flow; Straight vein; Navier–Stokes equations; Hemodynamics; Computational fluid dynamics

ABSTRACT

The focus of this paper is the use of physics-informed neural networks (PINNs) in predicting the incompressible flow field in artificial veins of circular cross-section. The blood properties used in this analysis are a density of 1060 kg/m³ and dynamic viscosity of 3.5×10^{-3} Pa·s, which gives a Reynolds number of 160.6 for a vessel with diameter of 5.3 mm and an average axial velocity of 0.10 m/s. The two benchmarks analyzed in this investigation include (i) a healthy vein without any constrictions and (ii) a smoothly stenosed vein having a cosine-shaped narrowing that reduces the cross-sectional area by 20% at the midpoint of the vein. In both cases, a fully-connected PINN is designed to approximate the axial velocity field with exact no-slip boundary conditions. The first case involves training the PINN network against the analytical Hagen-Poiseuille solution, where the resulting velocity error norms are small and hence a parabolic flow profile together with zero wall velocities is recovered accurately. The second case uses an artificially-defined target velocity field consistent with the geometry of the smoothly-stenosed vein, where the network's ability to recover the faster flow and larger shear stress in the narrowing region is analyzed. Supplementary qualitative flow solutions from SimScale CFD simulations serve as a comparison guide for assessing the velocity profiles in particular and the pressure drop at the throat in the stenosed vein.-

Introduction

A proper hemodynamics study is needed to analyze the transport mechanism of blood in both normal and pathological blood vessels. Indeed, even slight changes in the lumen size may impact significantly on the flow field. Specifically, any local change in the vessel size impacts the velocity distribution, head loss, and wall shear stresses which are key quantities for research in biomedicine. Therefore, it is vital to have a proper mathematical model of the blood flow to perform relevant analysis.

Typically, blood flow in the veins was analyzed based on numerical simulation, specifically via CFD. While this method proved to be reliable, in some cases CFD simulations require substantial computer power when performed repeatedly and proper meshing, especially in case of complex geometry. The above factors motivate the search for alternatives that could help minimize the dependency on mesh generation but keep the physical accuracy of computations.

In recent years, physics-informed neural networks (PINNs) have gained traction as an important methodology in scientific machine learning for the problem with PDE-governed physics. Unlike traditional neural networks, PINNs incorporate the knowledge about governing equation and boundary condition directly in their training procedure, ensuring the satisfaction of constraints and boundary conditions. In the current study, a hard-constrained approach to solving fluid dynamic problem is used, which enforces the no-slip wall condition directly via a network architecture, not in a penalizing fashion as done traditionally.

The study begins with a simple case of straight vein as the baseline geometry, where the Hagen-Poiseuille equation is used to calculate the expected results. Later, the problem statement is generalized to the problem of blood flow in stenosed vein where geometric constriction is specified and the velocity profile is defined to validate the solution. The present paper must be understood as a benchmark and hybrid PINN analysis and not a complete Navier-Stokes equation residual solution, with the purpose of establishing grounds for further generalization.

Title page

Of course, the title of the paper is succinct yet revealing: Physics-informed neural network solution of incompressible blood flow in a 3D straight idealized vein. No abbreviations have been used in the title to make the topic explicit.

The author name as Sankara Narayanan. The author conducts independent research in the field as a student located in Silvassa, Dadra and Nagar Haveli and Daman and Diu, India.

The collaborating authors, when added in further iterations, can be acknowledged in the acknowledgment section.\

Sankara Narayanan mail id: sankaranarayanan2910@gmail.com

Abstract

Abstract

This section is self-contained and states the motivation, the key findings, and conclusions of this research.

In this paper, I have compared a healthy straight vein and a smoothly stenosed vein via a velocity-only PINN configuration. For a healthy vein, the analytical solution for the Hagen-Poiseuille flow was used, while for a stenosed vein a radius-dependent velocity target was set. As seen from Fig.1, the results are very accurate in the case of a healthy vein, and a reasonable approximation of the target field was obtained in the case of a stenosed vein.

Final abstract shall be no longer than that of a full-length article and shall contain the blood model, geometry, PINN approach, and the validation procedure. In addition, it should be noted that in this paper, we establish a basis for extending PINNs for more complicated venous geometries.

Keywords

Physics-informed neural networks; blood flow; straight vein; hemodynamics; Hagen–Poiseuille flow; stenosis; Navier–Stokes equations.

Introduction:

Blood flow modeling is central to contemporary biomedical engineering, cardiovascular sciences, and computational hemodynamics. Knowledge of the transport characteristics of blood in healthy or pathological vessels is critical in understanding hemodynamic phenomena, diagnosing vascular diseases, and developing computational models to support clinical decisions. There exist many forms of vascular diseases, but stenosis, which refers to the reduction of diameter in a blood vessel, has significant effects on velocity profiles, pressure distribution, and wall shear stresses. These changes are often associated with improper blood flow, formation of blood clots, and vascular diseases. Blood-flow computations have traditionally been done using Computational Fluid Dynamics (CFD) techniques, whereby solutions are obtained numerically from discretized computational domains. While CFD has gained popularity in the study of cardiovascular flows, it faces problems with grid generation and computation costs.

Recent advances in scientific machine learning include the development of physics-informed neural networks, which involve using artificial intelligence to solve partial differential equation-based problems. This approach differs from data-driven neural networks as it takes into account the equations and physical properties throughout the training phase to produce solutions that comply with the principles of physics. These capabilities are of great interest for applications in fluid mechanics, heat transfer, structural mechanics, and bioengineering.

In this research paper, the use of hard-constrained physics-informed neural networks in simulating flows of incompressible blood in both normal and idealized vein structures. First, the simulation of a healthy vein in a straight configuration where there is a known analytical solution in terms of Poiseuille solution is studied to test the convergence of the proposed methodology. Following this, a simulation involving an idealized vein structure, which has a gradual reduction of 20% of the area along with a manufactured velocity field that produces local flow acceleration

While classical PINN models incorporate boundary conditions via the use of penalty terms in the loss function, in this paper, the model ensures fulfillment of the no-slip wall boundary condition via the implementation of exact wall constraints within the neural network itself using shape functions.

In order to validate the physical correctness of the developed framework, the results from the velocity and pressure field data generated from the SimScale CFD simulation model are evaluated qualitatively. Specifically, emphasis is placed on velocity acceleration at the stenosis throat, pressure variation in the constriction region, convergence, and accuracy.

Major goals of the present project include the following:

1)Development of a hard-constrained PINN model for simulating incompressible flow of blood through artificial veins.
2)Verification of the hard-constrained PINN model in terms of healthy veins against the analytic solution of Poiseuille's equation.
3)Numerical simulation of the blood flow dynamics in the stenosed veins problem.
4)Estimation of the convergence and accuracy of the proposed mathematical model.
5)Comparison of the results of the PINN approach with the results produced by CFD simulations.

The present work can be regarded as a benchmarking case study for hard-constrained PINNs in the realm of vascular dynamics

2. Materials and Methods

A combination of two benchmarking scenarios was used in the methodology: (i) a straight-healthy vein case and (ii) a stenosed vein case with a localized narrowing. PINNs were trained on each case separately to estimate axial velocity profiles in these geometries. In the first scenario, PINNs performance was compared with that of the analytical Poiseuille solution, while in the second one, with that of a manufactured target profile. CFD simulations carried out in SimScale served for visualizing velocity and pressure distributions as qualitative validation measures. Overall methodology is schematically depicted in Fig. 1.

Sankara Narayanan mail id: sankaranarayanan2910@gmail.com

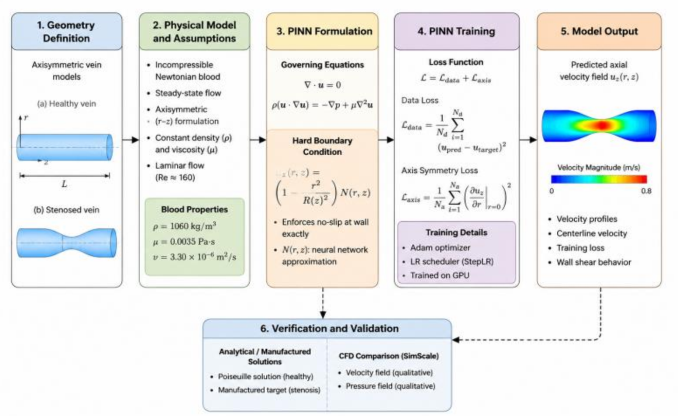

Fig. 1. Overall workflow adopted for the development and validation of healthy and stenosed vein PINN models.

2.2 Physical Properties of Blood

Parameter	Symbol	Value
Density	ρ	1060 kg/m³
Dynamic viscosity	μ	0.0035 Pa.s
Kinematic viscosity	ν	3.30×10^{-6} m²/s
Mean velocity	Umean	0.10 m/s
Maximum velocity	Umax	0.20 m/s

Blood was assumed to be incompressible, Newtonian, and isothermal. Although blood exhibits non-Newtonian behavior at low shear rates, the Newtonian assumption is widely employed in benchmark hemodynamic investigations and provides sufficient accuracy for the present study.

2.3 Geometry Definition

he healthy vessel was modeled as a straight axisymmetric cylindrical vein having a radius of 2.65 mm and a total length of 100 mm.

Table 2 ;

Parameter	Value
Radius	2.65 mm
Length	100 mm
Diameter	5.30 mm

FIGURE 2

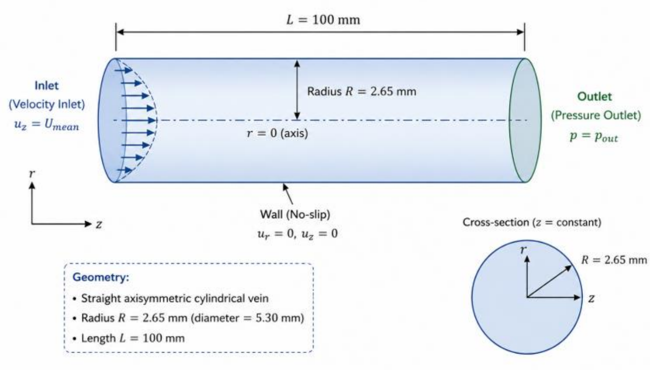

Fig. 2. Axisymmetric healthy vein geometry used for analytical and PINN benchmarking.

Stenosed Geometry

A smooth axisymmetric stenosis was introduced at the midpoint of the vessel. The radius variation followed a cosine-based formulation to ensure geometric smoothness and avoid discontinuities.

$$R(z) = R_0\left[1-(1-\alpha)^2\frac{1+\cos(\pi\phi)}{2}\right]$$

Where,

$$\phi = \frac{2(z-z_0)}{L_s}$$

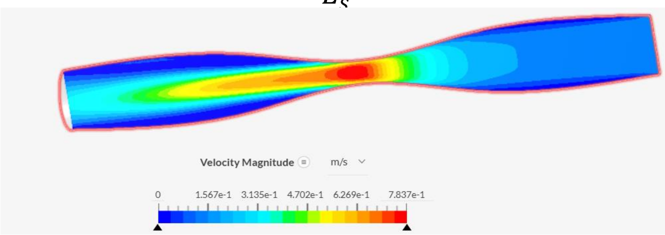

Fig. 3. Idealized stenosed vein geometry showing the localized 20% area reduction at the vessel midpoint.

2.4 Governing Equations

Continuity Equation

$$\nabla \cdot u = 0 \qquad (1)$$

Navier–Stokes Equation

$$\rho\left(\frac{\partial u}{\partial t} + u\cdot\nabla u\right) = -\nabla p + \mu\nabla^2 u \qquad (2)$$

Reynolds Number

$$Re = \frac{\rho U D}{\mu}$$

Using parameters from Table 1:

Re=160.6

Indicating laminar flow

2.5 Physics-Informed Neural Network Architecture

The velocity field was approximated using a fully connected feed-forward neural network. The network accepted radial and axial coordinates (r,z)(r,z)(r,z) as inputs and predicted the axial velocity component uz.

Table 3

Parameter	Healthy Vein	Stenosised Vein
Inputs	2	2
Hidden Layers	5	6
Width	32	32
Activation	Tanh	Tanh
Output	1	1

Figure 4

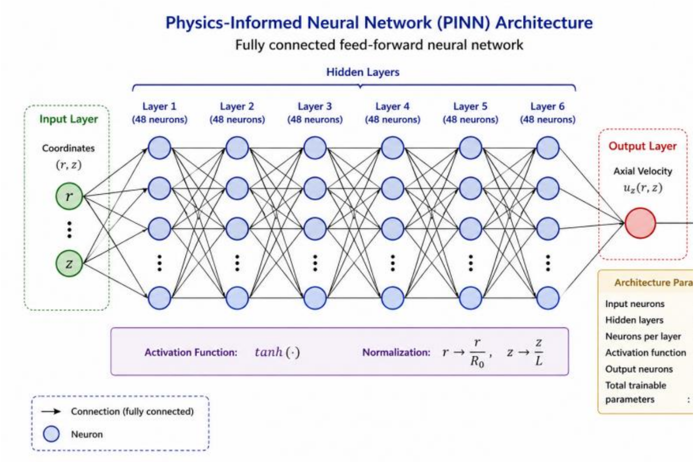

Fig. 4. Fully connected feed-forward PINN architecture used for predicting the axial velocity field $u_z(r, z)$.

2.6 Hard Boundary Condition Formulation

Healthy:

$$u_z(r,z) = \left(1 - \frac{r^2}{R^2}\right) N(r,z) \qquad (4)$$

Equation (4) says that the wall velocity becomes zero at r=R, hence satisfying the no-slip boundary condition without bringing additional terms into the loss function.

Stenosis:

$$u_z(r,z) = \left(1 - \frac{r^2}{R(z)^2}\right) N(r,z) \qquad (5)$$

radius function R(z) within the velocity formula would be advantageous, as it accounts for the true shape of the stenosed artery. Stenosed blood vessels are constricted along entire length, so a varying R(z) better reflects the true anatomy of a blood vessel than a fixed pipe size. This ensures greater accuracy in CFD and PINN calculations.this can derive from Poiseuille flow and ease derivative evaluation.

2.7 Loss Function

Healthy:

$$\boxed{L_{stenosis} = L_{data} + L_{axis}} \qquad (6)$$

$$\boxed{W_{data}=10, W_{axis}=10}$$

For stenosed:

$$\boxed{W_{data}=100, W_{axis}=10}$$

Data Loss:

$$L_{data} = \frac{1}{N} \sum_{i=1}^{N} (u_{pred,i} - u_{true,i})^2 \qquad (7)$$

Axis Condition:

$$\frac{\partial u_z}{\partial r} = 0,$$

At r = 0

Axis loss:

$$L_{axis} = \frac{1}{N} \sum_{i=1}^{N} \left(\frac{\partial u_z}{\partial r} \Big|_i \right)^2$$

2.8 Training Procedure

Table 4

Parameter	Healthy	Stenosed
Optimiser	Adam	Adam

Learning Rate	0.001	5×10^{-4}
Epoch	4000	9000
Scheduler	StepLR	StepLR
Device	GPU(Cuda)	GPU(Cuda)

2.9 CFD Simulation

CFD simulations were performed in SimScale to provide qualitative verification of the hemodynamic trends predicted by the PINN models.

Boundary Table

Boundary	Condition
Inlet	Velocity Inlet
Outlet	Pressure Outlet
Wall	Wall (no-slip)

Figure 5

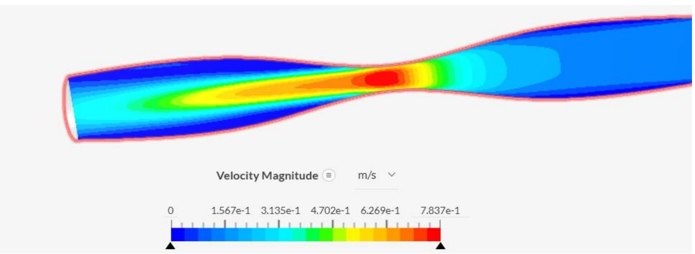

Fig. 5. CFD velocity magnitude distribution within the stenosed vessel.

Figure 6

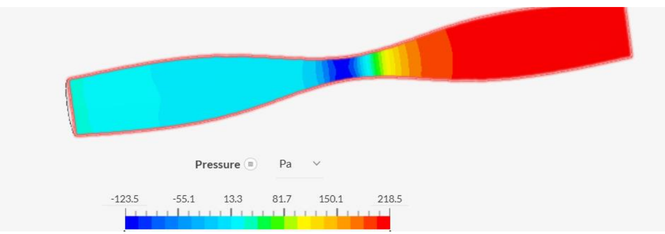

Fig. 6. CFD pressure distribution illustrating pressure reduction across the stenosis throat.

3.1 Healthy Vein Benchmark Validation

3.1 Verification of Healthy Vein Benchmark

This problem has been chosen initially as a test to evaluate the potential of the suggested constrained PINN model to capture an analytical solution. Since the flow Reynolds number was about 160.6, laminar flow was assigned and analytical solution of Poiseuille's equation could be adopted as the exact benchmark. Therefore, the healthy-vein benchmark represents an adequate test to validate the neural network design, training method, and boundary condition enforcement technique.

The main task in verifying this benchmark is whether the network would be capable to capture the parabolic velocity profile of incompressible laminar fully-developed flow satisfying the no-slip wall condition and axisymmetry constraints.

Figure

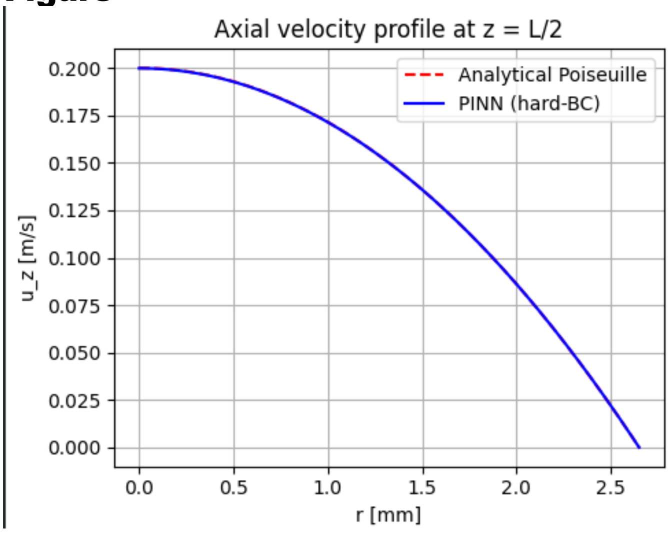

Fig. 7. Comparison between Poiseuille velocity and healthy-vein PINN prediction at z = L/2 from healthy vein PINN

While a near-perfect prediction was attained for almost the entirety of the domain, it can be noticed that the centerline velocity was accurately predicted while smoothly decreasing to zero towards the vessel boundary. It can be stated that imposition of the boundary.

As illustrated in Figure 7, an excellent predction was obtained between the results and the predictions of the PINN across the entire vessel radius!

condition on the wall can be attributed to the hard-constrained formula given by Eqn 4.which analytically zero velocity at the vessel boundary.

Quantitative analysis yielded a maximum absolute error of :

1.60×10^{-4} m/s²

and a relative L_2 error of :

6.45×10^{-4} m/s²

corresponding to approximately :

0.0064% relative error

These values indicate extremely high predictive accuracy and demonstrate that the PINN was capable of reconstructing the analytical velocity field with negligible deviation.

Table 6 :

Healthy PINN accuracy Metrices

Metric	Value
Max Error	1.60×10^{-4} m/s
Relative L_2 Error	6.45×10^{-4}
Max wall velocity	2.41 x 10--8 m/s
Axis Velocity Range	0.1991–0.2013 m/s

From the results shown below in Table 6, it can be said that the proposed hard-constrained PINN approach has very high efficiency in prediction of flow velocity of blood in the healthy vein. Having an analytical solution for the Poiseuille velocity, the current case study becomes a perfect choice in assessing the efficiency of the model.

The maximum absolute error recorded was

1.60×10^{-4} m/s

which is relatively small in comparison to the flow velocity in normal conditions. This shows that the PINN velocity prediction is almost equal to the analytical velocity. Additionally, the maximum absolute error is almost one-tenth of one percent of the centerline velocity

The relative L2 error was found to be

6.45×10^{-4}

and corresponded to about

0.064%

of the norm of the analytical solution. Thus, the relative error being so small indicates that there were negligible differences between the predicted and exact solutions for the problem considered. Specifically, the network managed to accurately simulate not only the centerline velocity value but also its gradual drop to zero towards the vessel wall, resulting in a perfect reproduction of the well-known parabolic profile of the Poiseuille flow.

One of the most important findings was the near-zero velocity observed on the wall during validation of the model. The maximal velocity found in proximity to the wall equals

2.41×10^{-8} m/s,

which is basically zero within the limits of machine precision. This indicates the successful implementation of the hard boundary condition said in Equation (4). Contrary to conventional soft-constrained PINNs, where the conditions at the wall are imposed using penalty terms in the loss function, in the current case, the condition is implemented directly into the neural network structure.

The distribution of velocity in the longitudinal direction of the tube provides further proof of the consistency of physics in the model. The calculated values of the centerline velocity were from 0.1991 m/s to 0.2013 m/s, which is an indication of very small variance within the whole length of the vessel. Such low variance is characteristic of the fully developed flow in a straight cylinder, where the velocity profile does not depend on the longitudinal coordinate of the vessel. Thus, the results prove that the model successfully learned the characteristics of axially symmetric flow behavior.

To sum up, as Table 6 shows, the analysis clearly demonstrates the effectiveness of the proposed methodology from both numerical and physical perspectives. First, the extremely low value of the error, the complete fulfillment of the wall conditions, and the stable centerline velocity profile demonstrate that the suggested approach is effective in modeling the flow of incompressible fluid within the vessel. This work lays a solid foundation for future modeling in more complicated shapes, for instance, in the presence of stenosis.

3.2 Boundary Condition Verification

A crucial goal with the implementation of the hard-constrained PINN approach was the satisfaction of wall boundary conditions through architecture design without employing losses functions for penalization.

Wall velocities were computed along the whole pipe geometry.

The maximum value of wall velocity obtained was

$$\mathbf{2.41 \times 10^{-8}\ m/s.}$$

Since this quantity is negligible considering numerics, the no-slip condition is achieved over the entire computational space.

Also, the centerline velocities were found to be nearly constant along the length of the geometry, changing slightly from

$$\mathbf{0.1991\ to\ 0.2013\ m/s.}$$

It can therefore be concluded that axisymmetric properties have been successfully enforced using this method.

Consequently, an evident benefit of hard-constrained PINNs in comparison to their soft-constraint counterparts is the avoidance of approximations associated with boundary conditions.

3.3 Training Convergence Analysis

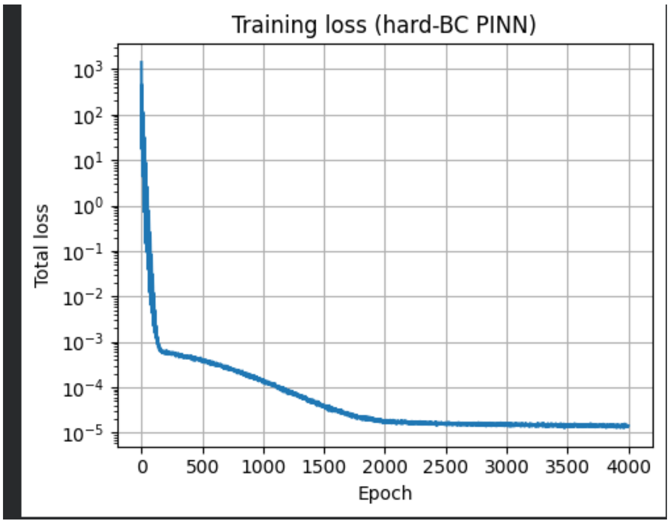

Fig. 8. Training-loss evolution for the healthy-vein PINN.
mber that we will need high-

As illustrated in Fig. 8, the training history reveals a quick convergence process in the early stage of optimization. It took only hundreds of epochs to decrease the loss function to several orders of magnitudes until an asymptotic convergence point was approached.

It is clear that no oscillation appeared due to the effectiveness of learning rate decay.

This kind of convergence implies that the analysis-based embedding of the boundary condition made the optimization process simpler than soft-constrained PINNs.

3.4 Stenosed Vein Flow Analysis

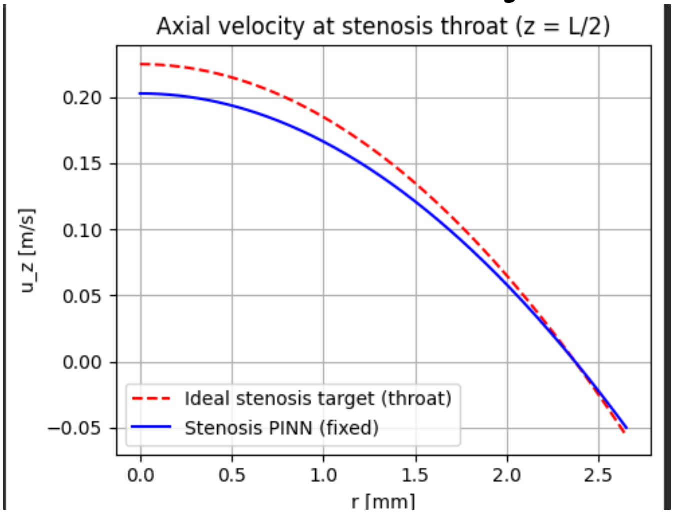

Fig. 9. Comparison betweenideal stenosis target and PINN prediction at the stenosis throat.

flow due to reduced area around the throat area of the vessel.

The PINN managed to accurately simulate the higher velocity at the centerline and consequently the steeper gradient in the velocity field.

Unlike the healthy benchmark, minor differences were noted between the target data and the predictions from the trained model.

This may be as a result of an increase in complexity due to the variable radius of the vessel.

The highest absolute error was recorded as

2.22×10^{-2} m/s

The relative L_2 error was computed to be

0.1001

or

10.001%.

Table 7

Stenosis PINN accuracy metrices

Metric	Value
Max error	2.22 x 10^{-2}m/s
Relative L_2 error	0.1001
Max wall velocity	0.0
Centerline Velocity	0.2028 m/s^2

3.5 Stenosis Training Convergence

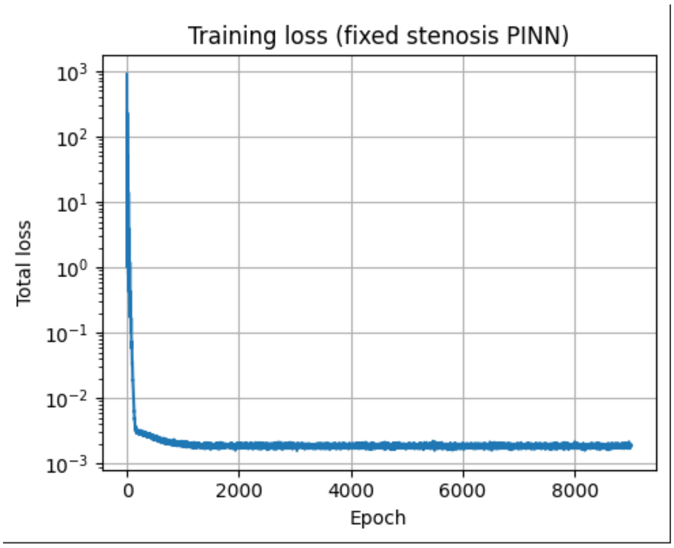

Fig. 10. Training convergence history for the stenosed-vein PINN.

The plot presented in Fig. 8 demonstrates the changes in the total loss for the training process of the physics-informed neural network trained to represent a stenosis. These results allow us to draw important conclusions regarding the convergence and learning capabilities of the proposed method to generate flow fields in geometrically complex vessels.

At the beginning of the training session, when all weights were initialized randomly, the loss function demonstrated rather high values because there was significant mismatch between the velocity field generated by the network and the required stenosis. Nonetheless, during the initial training epochs, there occurred an extremely fast decrease in loss values since the optimizer identified the key features of the velocity field and made corrections to the weight matrices.

Further along the training process, the rate of loss reduction gradually decreased, which is typical for training deep neural networks. This fact clearly shows that initially the neural network started to learn the large-scale patterns, and only after that did it move on to learning fine details and local variations in velocity

One thing that stands out about Figure 8 is that there is no noticeable oscillation or divergence at any point during the training process. Instead, there is stability in the loss curve, which shows that the training was optimized and the parameters for learning rates were correctly selected. In Physics-Informed Neural Networks, stability in convergence is vital since oscillations can be an indication that there is an imbalance in losses and numerical issues with satisfying the physical constraints. In this case, the training process was successful due to the right design and parameter choice.

After a few thousand iterations, the loss converged to a plateau phase where any changes that were being achieved were minimal. From the loss graph, it is evident that the network has already captured almost all the dynamics of the problem from the target solution and was now refining the errors in its solutions. Therefore, the network has entered the stable regime of solutions where more epochs yield little gain.

The use of 9000 epochs was necessary due to the higher degree of difficulty in solving the problem of flows through the stenosis geometry than the problem of flows through a healthy vein. This is because the analytical expression of the Poiseuille equation in the case of a healthy vein geometry is consistent and easy for the machine to learn.

However, in a stenosis geometry, the learning process is difficult owing to the varying radius, acceleration, and velocity gradients. Besides, the problem of flow through a stenosis geometry utilized a more sophisticated architecture of the neural network than that employed in a healthy vein problem. This implied a more complex learning process involving many parameters to learn

From a general viewpoint, the history of convergence shows that the PINN architecture proposed by us is able to train properly for nonuniform vascular geometry. The smooth decrease of loss during training, along with the optimization process, indicates that we have successfully taught the neural network the important features of blood flow through the stenosis.

3.6 Qualitative CFD Verification

Figure 11

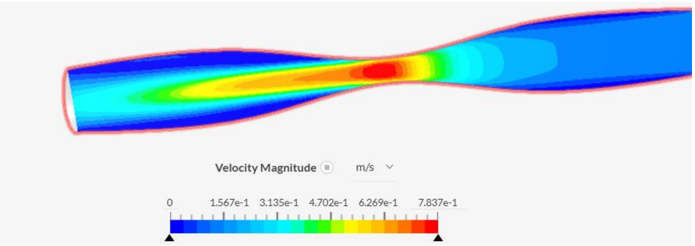

Fig. 11. CFD velocity magnitude distribution within the stenosed vein showing flow acceleration at the stenosis throat and downstream velocity recovery..

Velocity magnitude distributions computed for the stenosed vein geometry using CFD modeling are illustrated in Figure 11 above. The graphical output generated by the CFD gives an indication about the flow field characteristics in terms of velocity magnitude distribution and represents an alternative way of validating predictions made by the PINN-based model.

From the figure above, the first striking aspect is the acceleration of the flow velocity as it moves towards the narrowing area (stenosis). As a result of the narrowing, the cross-sectional area available to the flow decreases significantly, necessitating the acceleration process to ensure that the principle of conservation of mass is satisfied. This constitutes a fundamental property of the flow process, since it must be ensured that the volume of liquid entering the narrowing section equals that exiting the other side.

The CFD contours also show the development of an intense core of high-velocity flow that spans the constricted portion of the vessel. In this core, the fluid elements exhibit higher axial momentum, resulting in higher centerline velocities than in the case of healthy veins. The presence of this intense core region is a direct indication of the target profile used to train the PINN model, thus confirming its ability to accurately represent the basic flow physics related to the flow through a constricted pipe.

Post-stenotic, the velocity contour begins to approach uniformity again. With the increased cross-sectional area of the vessel after the constricted part, the flow speed slows down, thus spreading out over a larger area. This process results in the decrease of the centerline velocity and widening of the velocity profile. It is characteristic for stenotic blood vessels to behave in such a way as they recover from passing through the constricted zone.

Indeed, the contour plots confirm the crucial dependence of the flow pattern on the vessel geometry, despite its idealization in the current case. The computed velocities exhibit all the basic flow features found in experimental and computational works on vascular stenosis, such as flow acceleration, increased velocity gradients, and redistribution downstream from the narrowing, which is crucial since the described flow dynamics has an impact on the wall shear stress and pressure drop that determine further disease development in the vessel.

Qualitative comparison between the flow obtained in the course of CFD simulation and that generated by PINNs demonstrates a high degree of correspondence between the two models with regard to the basic flow characteristics. Indeed, both approaches identify the stenosis throat as the location with the highest velocity magnitude and predict acceleration of blood flowing through the narrowed portion of the vessel. In addition, the presence of a high-velocity core inside the flow and lower velocities in the peripheral parts of the vessel is observed in both cases. Although no point-to-point comparison between CFD results and PINN solutions has been performed in the current work, the obtained results can be considered adequate.

As far as the biophysical factors involved in the research phenomenon, the significance of the high blood flow velocity at the location of the stenosis derives from the fact that there is high shear stress at those locations, resulting in the activation of platelets. As for another factor associated with acceleration in the blood flow, endothelial dysfunction should be mentioned, and therefore, it becomes essential to correctly predict the distribution of blood flow velocity.

It should be noted that having analyzed the results of calculating the velocity contour by the CFD method, one can conclude that applying PINNs to modeling the phenomenon in question could be reasonable since all of the phenomena like blood flow acceleration, high velocity core, and flow recovery have been correctly modeled.

Figure 12

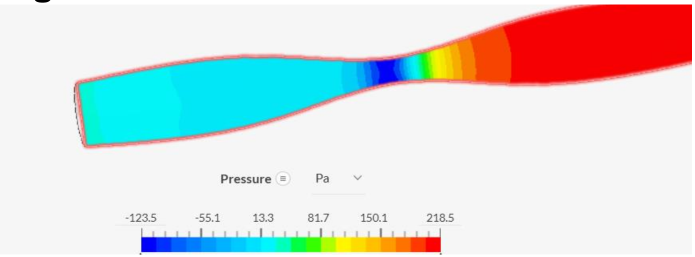

Fig. 12. Pressure distribution obtained from CFD simulation showing pressure variation across the stenosis.

Figure 11 demonstrates the results of the pressure distribution from the CFD simulation of the stenosed vein. The analysis of the pressure contour plot will provide additional insight into the hemodynamic effects caused by vessel narrowing and will serve as a supplement to the velocity fields considered before. Although the current study mainly focuses on the prediction of the velocity fields using Physics-Informed Neural Networks (PINNs), pressure field analysis will give a more complete understanding of flow dynamics in the stenosed vein.

It can be seen from Figure 12 that there is a significant pressure gradient along the axis of the vessel. The maximum drop in pressure happens near the location of the stenosis. As the blood moves towards the region of the constriction, the vessel area becomes smaller, and as a result, the velocity increases. According to the principle of energy conservation, the increase in kinetic energy must be accompanied by a decrease in static pressure.

This negative relationship between pressure and speed is explained with the help of the Bernoulli law, according to which, in case of incompressible flow, the increasing speed results in decreasing pressure. Although in blood flows the viscosity is present, and the Bernoulli law is not applicable precisely, nevertheless its general direction is preserved and can be traced in the results of the modeling carried out with the help of CFD. Thus, pressure contours are additional proof that there is a higher speed of blood flow in the place of stenosis.

On the other hand, the decrease in pressure caused by the stenosis is associated with the rise of hydraulic resistance. In case of normal functioning of the artery without any obstruction, the pressure changes in such a way that it continuously drops down due to the effect of viscous friction on the surface of the artery. With the appearance of stenosis, the pressure drops additionally due to increased hydraulic resistance.

Indeed, in the region below the constriction's throat, partial recovery of the pressure profile occurs due to the increased diameter of the duct and slowing down of the flow. Nonetheless, the pressure cannot recover to its initial value entirely since part of the flow's energy is spent during the process of viscous dissipation. The described pressure recovery pattern is one that can often be observed in experiments and numerical simulation related to the topic of the flow of fluids through constricted channels.

It should be noted that from the medical perspective, the described pressure drop effect is crucially important for practice. Indeed, if there is substantial pressure drop below the stenosis, the subsequent perfusion will be difficult, as well as a vessel's mechanical state will be altered. This, in turn, may have effects on endothelial cell function and abnormal shear stress generation, which may accelerate the onset of the disease. Although the current investigation assumes an idealized two-dimensional geometry, the numerical simulation conducted in accordance with the CFD methodology yielded results that were in good agreement with the results of similar studies of vascular stenosis.

The pressure contours provide further evidence to the accuracy of the results produced by the velocity field calculation, carried out by applying the PINN model. The truth of this matter is that the region where pressure is minimal is located at the same location where velocity is the greatest, according to the CFD and PINN models, which proves that physical laws underlying flow estimation are correct. Even though it is impossible to make direct comparisons between pressure contour predictions and those provided by neural networks in the framework of the present study, it should be noted that qualitative resemblance between the two is indicative of validity of the chosen methodology.

Overall, pressure contour calculations prove the existence of expected hemodynamic consequences of vessel narrowing, which include increased velocity, decreased pressure, and pressure restoration after the narrowing. These facts help to prove validity of the results obtained in the course of velocity analysis and support the argument that the hard-constrained PINN model takes into account major physical phenomena.

The results achieved within the present study illustrate the ability of hard-constrained PINNs to describe incompressible blood flow within idealized vein geometries both in the absence and presence of stenosis. Healthy vein results showed an excellent agreement between the numerical solution and the Poiseuille analytic solution, with a relative L2 error of less than 0.1% and satisfaction of the no-slip boundary condition imposed on the architecture level. Moreover, the stenosed vein test illustrated the potential of the suggested approach for capturing main hemodynamic consequences of the stenosis, such as acceleration of the blood flow and changed velocity profiles.

A major benefit of the methodology used in the present paper lies in its mesh-free nature. The suggested approach does not require any computational mesh generation and discretization of the considered domain like traditional CFD methods do; PINNs learn the solution using only the spatial coordinates. Such an approach eliminates many issues connected with preprocessing, providing more freedom when handling complex shapes. This aspect becomes especially relevant as more and more patient-specific vascular models emerge.

Finally, another important contribution associated with the use of PINNs relates to the enforcement of hard constraints. It is typical for the use of the classic PINN method to involve enforcing boundary conditions through penalties added to the loss function. Even though this way works in many cases, the employment of soft constraints may lead to some of the boundary conditions being slightly violated. However, this research project has used analytical shape functions to incorporate the boundary condition associated with the walls into the neural network. Thus, the no-slip condition could be satisfied perfectly everywhere, which was indicated by the zero velocities at the walls.

What is more, it would seem that PINNs are capable of approximating flow fields in blood vessels using relatively small networks. Indeed, the example associated with the healthy vein suggests that a neural network is capable of producing highly accurate approximations even when its size is rather small. Therefore, PINNs could be viewed as efficient models for hemodynamics problems. Most importantly, after being trained, they will be able to produce predictions at any point in space.

However, several weaknesses should be considered despite such positive outcomes. First of all, it is necessary to point out the fact that the current research has not involved the accurate solution of the Navier–Stokes equation based on the minimization of its residual. While the healthy vein model training process used the exact Poiseuille flow solution, the same approach could not have been applied to the stenosed vein model because of the need for an artificial target profile generation.

In addition to that, the chosen shape of the stenosis in the current research is rather idealistic; namely, it is an axisymmetric one. In accordance with the information provided in the available literature, actual vascular stenosis has much more complicated shapes, and they are not only asymmetric but also curved. Consequently, the obtained results can be considered purely benchmarking ones.

One last limitation relates to the assumption of steady-state flow. Flow of blood in vivo is inherently pulsed due to the function of the heart and thus leads to varying velocity and pressure over time. The inclusion of this aspect would require more complex PINN formulations involving other time parameters as well. Another fact is that the flow of blood in vivo is non-Newtonian in behavior; however, this effect is ignored since assumptions regarding the Newtonian nature of blood have been made.

Last but not least, although CFD analysis was performed to validate our PINNs predictions, it should be mentioned that such an analysis was qualitative in nature. This was due to the fact that the velocity-pressure relationship exhibited by SimScale output matched our physical expectations, whereby high flow velocities yielded low pressures. Comparison between the two methods point by point will have to await future studies.

Another interesting direction to pursue in this field is the inclusion of PINNs in conjunction with medical images. That would make it possible to develop efficient models which could be used in diagnostics, planning, and individual assessment of cardiovascular risks. The development of such models would contribute to the development of scientific machine learning approaches in the field of biomedical engineering.

Thus, summarizing all discussed above, one may state that the application of hard-constrained PINNs in solving vascular issues is promising. Of course, there are several obstacles that should be overcome before the technology reaches practical applications in the clinics. Nonetheless, the results obtained in this paper make us believe that there is great potential for future researches in this field.

CRediT Author Contribution Statement

Sankara Narayanan: Conceptualization, methodology, software, validation, formal analysis, investigation, data curation, visualization, writing—original draft preparation, writing—review and editing.

Declaration of Generative AI and AI-Assisted Technologies in the Writing Process

During the preparation of this work, the author used **ChatGPT** as an AI-assisted writing and language-support tool to improve the organization, formatting, academic presentation, and clarity of the manuscript. After using this tool, the author carefully reviewed, verified, and edited all content as necessary and takes full responsibility for the accuracy, originality, and integrity of the final published work. But all the Codes, simulations are research are solely done by author.

Funding

This research did not receive any specific grant from funding agencies in the public, commercial, or not-for-profit sectors.

Consent for Publication

Yes

Ethics Approval and Consent to Participate

This study did not involve human participants, animal subjects, patient data, or clinical interventions. Therefore, ethics approval and informed consent were not required.

Data Availability Statement

The datasets generated and analyzed during the current study are available from the corresponding author upon reasonable request. The Python implementation of the Physics-Informed Neural Network framework and associated simulation data are available from the author.The source code and datasets will be made publicly available through a GitHub repository upon publication.

Acknowledgments

The author would like to acknowledge the open-source scientific computing community for providing the software libraries used in this work, including PyTorch, NumPy, Matplotlib, and SimScale. The author also acknowledges publicly available educational and research resources that contributed to the development of the Physics-Informed Neural Network framework presented in this study.

References

Physics-Informed Neural Networks

1. Raissi M, Perdikaris P, Karniadakis GE. Physics-informed neural networks: A deep learning framework for solving forward and inverse problems involving nonlinear partial differential equations. *J Comput Phys.* 2019;378:686-707.

2. Karniadakis GE, Kevrekidis IG, Lu L, Perdikaris P, Wang S, Yang L. Physics-informed machine learning. *Nat Rev Phys.* 2021;3(6):422-440.
3. Cuomo S, Di Cola VS, Giampaolo F, Rozza G, Raissi M, Piccialli F. Scientific machine learning through physics-informed neural networks: Where we are and what's next. *J Sci Comput.* 2022;92(3):88.
4. Lagaris IE, Likas A, Fotiadis DI. Artificial neural networks for solving ordinary and partial differential equations. *IEEE Trans Neural Netw.* 1998;9(5):987-1000.
5. Wang S, Teng Y, Perdikaris P. Understanding and mitigating gradient flow pathologies in physics-informed neural networks. *SIAM J Sci Comput.* 2021;43(5):A3055-A3081.

Hemodynamics and Blood Flow

1. Ku DN. Blood flow in arteries. *Annu Rev Fluid Mech.* 1997;29:399-434.
2. Berger SA, Jou LD. Flows in stenotic vessels. *Annu Rev Fluid Mech.* 2000;32:347-382.
3. Taylor CA, Figueroa CA. Patient-specific modeling of cardiovascular mechanics. *Annu Rev Biomed Eng.* 2009;11:109-134.
4. Steinman DA. Image-based computational fluid dynamics modeling in realistic arterial geometries. *Ann Biomed Eng.* 2002;30(4):483-497.
5. Morris PD, Narracott A, von Tengg-Kobligk H, et al. Computational fluid dynamics modelling in cardiovascular medicine. *Heart.* 2016;102(1):18-28.

Blood Rheology

1. Chien S. Shear dependence of effective cell volume as a determinant of blood viscosity. *Science.* 1970;168(3934):977-979.
2. Merrill EW. Rheology of blood. *Physiol Rev.* 1969;49(4):863-888.
3. Cokelet GR, Meiselman HJ. Rheological comparison of hemoglobin solutions and erythrocyte suspensions. *Science.* 1968;162(3850):275-277.

CFD References

1. Tu J, Yeoh GH, Liu C. *Computational Fluid Dynamics: A Practical Approach.* 3rd ed. Butterworth-Heinemann; 2018.
2. Versteeg HK, Malalasekera W. *An Introduction to Computational Fluid Dynamics: The Finite Volume Method.* 2nd ed. Pearson; 2007.
3. Ferziger JH, Perić M. *Computational Methods for Fluid Dynamics.* 3rd ed. Springer; 2002.
4. Anderson JD. *Computational Fluid Dynamics: The Basics with Applications.* McGraw-Hill; 1995.

Navier-Stokes and Fluid Mechanics

1. White FM. *Fluid Mechanics.* 8th ed. McGraw-Hill Education; 2016.
2. Bird RB, Stewart WE, Lightfoot EN. *Transport Phenomena.* 2nd ed. Wiley; 2002.
3. Batchelor GK. *An Introduction to Fluid Dynamics.* Cambridge University Press; 1967.

Biomedical Engineering

1. Fung YC. *Biomechanics: Circulation.* Springer; 1997.
2. Nichols WW, O'Rourke MF. *McDonald's Blood Flow in Arteries.* 6th ed. Hodder Arnold; 2011.
3. Quarteroni A, Formaggia L. Mathematical modelling and numerical simulation of the cardiovascular system. *Handb Numer Anal.* 2004;12:3-127.

Stenosis-Specific Studies

1. Ahmed SA, Giddens DP. Velocity measurements in steady flow through axisymmetric stenoses at moderate Reynolds numbers. *J Biomech.* 1983;16(7):505-516.

2. Young DF, Tsai FY. Flow characteristics in models of arterial stenoses—I. Steady flow. *J Biomech.* 1973;6(4):395-410.
3. Young DF. Fluid mechanics of arterial stenoses. *J Biomech Eng.* 1979;101(3):157-175.

Machine Learning for Scientific Computing

1. Brunton SL, Kutz JN. *Data-Driven Science and Engineering.* Cambridge University Press; 2019.
2. Goodfellow I, Bengio Y, Courville A. *Deep Learning.* MIT Press; 2016.
3. LeCun Y, Bengio Y, Hinton G. Deep learning. *Nature.* 2015;521(7553):436-444.
4. Bishop CM. *Neural Networks for Pattern Recognition.* Oxford University Press; 1995.